Long-range hybrid network with point and distributed Brillouin sensors using Raman amplification

Ander Zornoza*, Rosa Ana Pérez-Herrera, César Elosúa, Silvia Diaz, Candido Bariain, Alayn Loayssa, Manuel Lopez-Amo

Universidad Pública de Navarra,Campus Arrosadía s/n, 31006 Pamplona,SPAIN
**ander.zornoza@unavarra.es*

Abstract: We propose a novel concept for hybrid networks that combine point and distributed Brillouin sensors in a cost-effective architecture that also deploys remote distributed Raman amplification to extend the sensing range. A 46-km proof-of-concept network is experimentally demonstrated integrating point vibration sensors based on fiber Bragg gratings and tapers with distributed temperature sensing along the network bus. In this network the use of Raman amplification to compensate branching and fiber losses provides a temperature resolution of 0.7°C and 13 m. Moreover, it was possible to obtain good optical signal to noise ratio in the measurements from the four point vibration sensors that were remotely multiplexed in the network. These low-cost intensity sensors are able to measure vibrations in the 0.1 to 50 Hz frequency range, which are important in the monitoring of large infrastructures such as pipelines.

OCIS codes: (280.4788) Optical sensing and sensors; (060.2370) Fiber optics sensors (290.5860) Scattering, Raman; (290.5830) Scattering, Brillouin; (120.7280) Vibration analysis

References and links

1. H.-N. Li, "Recent applications of fiber optic sensors to health monitoring in civil engineering," Eng. Structures **26**(11), 1647–1657 (2004).
2. A. Rogers, "Handbook of fibre optic sensing technology", ed. J. M. Lopez-Higuera (John Wiley & Sons, Chichester, 2002), Chap. 14.
3. A. D. Kersey, "Optical Fiber Sensors: Applications, analysis and future trends", ed. J. Dakin and B. Culshaw (Artech House, Boston, 1997), Chap. 15.
4. J. D. C. Jones, and R. McBride, "Optical fiber sensor technology: Devices and technology", ed. K. T. V. Grattan and B. T. Meggit, (Chapman & Hall, London, 1998), vol. 2, p. 117.
5. M. Niklès, "Fibre optic distributed scattering sensing system: Perspectives and challenges for high performance applications," Proc. SPIE **6619**, 66190D (2007).
6. M. N. Alahbabi, Y. T. Cho, and T. P. Newson, "150-km-range distributed temperature sensor based on coherent detection of spontaneous Brillouin backscatter and in-line Raman amplification," J. Opt. Soc. Am. B **22**(6), 1321–1324 (2005).
7. E. Tapanes, "Fibre optic sensing solutions for real-time pipeline integrity monitoring," presented at the Australian Pipeline Industry Association National Convention (2001), http://www.iceweb.com.au/Newtech/FFT_Pipeline_Integrity_paper.pdf
8. P. Datta, I. R. Matías, C. Aramburu, A. Bakas, J. M. Otón, and M. López-Amo, "Tapered optical-fiber temperature sensor," Microw. Opt. Technol. Lett. **11**(2), 93–95 (1996).
9. C. Bariáin, I. R. Matías, F. J. Arregui, and M. López-Amo, "Experimental results towards development of humidity sensors by using a hygroscopic material on biconically tapered optical fibre," Proc. SPIE **3555**, 95–105 (1999).
10. F. J. Arregui, I. R. Matias, C. Bariain, and M. Lopez-Amo, "Experimental design rules for implementing biconically tapered single mode optical fibre displacement sensors," Proc. SPIE **3483**, 164–168 (1998).
11. C. Elosua, I. R. Matias, C. Bariain, and F. J. Arregui, "Volatile Organic Compound Optical Fiber Sensors: A Review," Sensors **6**(11), 1440–1465 (2006).
12. S. Diaz, S. Abad, and M. Lopez-Amo, "Fiber Optic Sensor Active Networking with Distributed Erbium Doped Fiber and Raman Amplification," Laser Photon. Rev. **2**(6), 480–497 (2008).

#123929 - $15.00 USD Received 8 Feb 2010; revised 6 Apr 2010; accepted 6 Apr 2010; published 22 Apr 2010

13. S. Diaz, G. Lasheras, and M. López-Amo, "WDM bi-directional transmission over 35 km amplified fiber-optic bus network using Raman amplification for optical sensors," Opt. Express **13**(24), 9666–9671 (2005), http://www.opticsinfobase.org/oe/abstract.cfm?URI=oe-13-24-9666.
14. V. Lecœuche, D. J. Webb, C. N. Pannell, and D. A. Jackson, "25 km Brillouin based single-ended distributed fibre sensor for threshold detection of temperature or strain," Opt. Commun. **168**(1-4), 95–102 (1999).
15. A. Zornoza, D. Olier, M. Sagues, and A. Loayssa, "Distortion-free Brillouin distributed sensor using RF shaping of pump pulses," Proc. SPIE **7503**, 75036D (2009).
16. A. Minardo, R. Bernini, L. Zeni, L. Thevenaz, and F. Briffod, "A reconstruction technique for long-range stimulated Brillouin scattering distributed fibre-optic sensors: Experimental results," Meas. Sci. Technol. **16**(4), 900–908 (2005).
17. S. Diaz, S. Foaleng-Mafang, M. Lopez-Amo, and L. Thévenaz, "A high-performance optical time-domain brillouin distributed fiber sensor," IEEE Sens. J. **8**(7), 1268–1272 (2008).
18. D. Alasia, M. G. Herráez, L. Abrardi, S. M. López, and L. Thévenaz, "Detrimental effect of modulation instability on distributed optical fibre sensors using stimulated Brillouin scattering," Proc. SPIE **5855**, 587–590 (2005).
19. N. Linze, W. Li, and X. Bao, "Signal-to-noise ratio improvement in Brillouin sensing," Proc. SPIE **7503**, 75036F (2009).
20. Y. D. Gong, "Guideline for the design of a fiber optic distributed temperature and strain sensor," Opt. Commun. **272**(1), 227–237 (2007).
21. M. A. Soto, G. Bolognini, F. Di Pasquale, and L. Thévenaz, "Distributed strain and temperature sensing over 50 km of SMF with 1 m spatial resolution employing BOTDA and optical pulse coding" Proc. SPIE 7503, PDP09 (2009)
22. J. Bromage, P. J. Winzer, and R. J. Essiambre, "Multiple path interference and its impact on system design", in Raman Amplifiers for Telecommunications **2**, M. N. Islam, ed. (Springer, 2004), Chap. 15.
23. L. Grüner-Nielsen, and Y. Qian, "Dispersion-compensating fibers for Raman applications," in Raman Amplifiers for Telecommunications 1, M. N. Islam, ed. (Springer, 2004), Chap. 6.
24. I. R. Matías, C. Fernandez-Valdevieso, F. J. Arregui, C. Bariain, and M. Lopez-Amo, "Transmitted Optical Power through a Tapered Single-Mode Fiber Under Dynamic Bending Effects," Fiber Integrated Opt. **22**(3), 173–187 (2003).
25. S. Lacroix, R. Bourbonnais, F. Gonthier, and J. Bures, "Tapered monomode optical fibers: understanding large power transfer," Appl. Opt. **25**(23), 4421–4425 (1986).

1. Introduction

Structural health monitoring has attracted much attention in both research and development in recent years. This reflects an increasing need to control the continuous deterioration conditions of important civil infrastructures, such as buildings, tunnels, dams, bridges, piles and pipelines [1]. Distributed fiber optic sensors are particularly suitable for large structural monitoring applications since all the segments of an optical fiber act as sensors and therefore the perturbations within various segments of the structure can be sensed [2]. Their electromagnetic immunity and their dielectric structure also make them ideal for use in harsh environments, like those in the oil and gas and electrical industries [1–4].

Distributed fiber optic sensors are based on the modulation of light intensity in the fiber. The three major distributed sensor techniques are: optical time domain reflectometry based on Rayleigh backscattering, which has been extensively deployed to measure the attenuation profiles of fiber optic links, and sensors based on Raman and Brillouin scattering. Raman scattering is used for distributed temperature measurement because it is based on the detection of light scattered by molecular vibrations that depend on this measurand. However, distributed Raman sensors require the use of multimode fibers to maximize the detected spontaneous Raman scattering signal, which limits its maximum useful range to below 10km. Distributed sensors based on Brillouin scattering have greater potential because of several advantages [5]. First, Brillouin scattering can be stimulated by the use of a probe wave, thus higher signal to noise ratios are attainable. Moreover, long distance measurements are possible because standard low-loss singlemode fibers are used and optical amplification can be deployed to further enhance of the reach of these systems [6]. Finally, distributed sensors based on Brillouin scattering are the most complete technique because they provide simultaneous information of temperature and strain along the length of a standard low-cost telecommunications optical fiber [2].

#123929 - $15.00 USD Received 8 Feb 2010; revised 6 Apr 2010; accepted 6 Apr 2010; published 22 Apr 2010

Therefore, by wrapping or embedding a fiber inside a structure and using distributed Brillouin scattering sensing, users can detect when an structure is being abnormally strained or heated/cooled, e.g. because of leakage in a pipe, allowing problems to be corrected before catastrophic failure occurs. However, many other measurements apart from strain and temperature are needed in the practical monitoring of large infrastructures, for instance, gas concentrations or vibrations. Particularly, the detection of low frequency vibrations (from 50Hz to 0.1 Hz) needs to be monitored in pipelines, civil structures, buildings, etc [1,7]. Distributed fiber optic sensing systems do not carry out these last mentioned measurements, whereas local (or point) fiber optic sensors are well suited for these tasks. For example, fiber-optic-taper based sensors employed as transducers are able to measure a number of environmental parameters [8–10] or gases [11]. They show distinct advantages such as their simple fabrication process, low-cost and versatility in the number of measurable parameters. Furthermore, long-range sensing networks for point sensors are now possible using Er-doped fiber or Raman optical amplification [12]. For instance, taper-based point temperature sensors using fiber Bragg gratings as wavelength reference elements have been multiplexed at distances up to 35 km [13].

In this work we propose another step in the development of long-range sensing networks: the integration, for the first time to our knowledge, of point and distributed sensors in a hybrid consolidated long multiplexing network. This offers obvious advantages as the fiber lengths that are anyway needed to interconnect and multiplex point sensors also serve as distributed sensors. However, there are significant challenges to overcome in order to implement these networks as the increased complexity of the sensor system can lead to problems such as crosstalk, Rayleigh backscattering overlapping the sensors signals or limitations in the sensor range imposed by the interplay of the different signals present. Moreover, in any case it becomes necessary to optimize the operating parameters of all sensors involved so that satisfactory performance is obtained for all of them simultaneously.

Here, we experimentally demonstrate a 46 km hybrid sensor network integrating point vibration sensors based on fiber optic tapers with distributed temperature sensing based on stimulated Brillouin scattering. The Brillouin distributed sensing sub-system is specially tailored for long distance sensing, utilizing a novel method to generate the sensing signals that minimizes systematic measurement errors. Furthermore, Raman distributed amplification is deployed to simultaneously amplify both the Brillouin sensing and the interrogation signals of the point sensors. This simultaneously increases the range of the Brillouin distributed sensor and enhances the optical signal to noise ratio (OSNR) of the point sensor system.

2. Description of the sensor network

Figure 1 schematically depicts the hybrid sensor network that we proposed. The system can be separated in two parts: the sensor network itself and the monitoring station equipment.

#123929 - $15.00 USD Received 8 Feb 2010; revised 6 Apr 2010; accepted 6 Apr 2010; published 22 Apr 2010

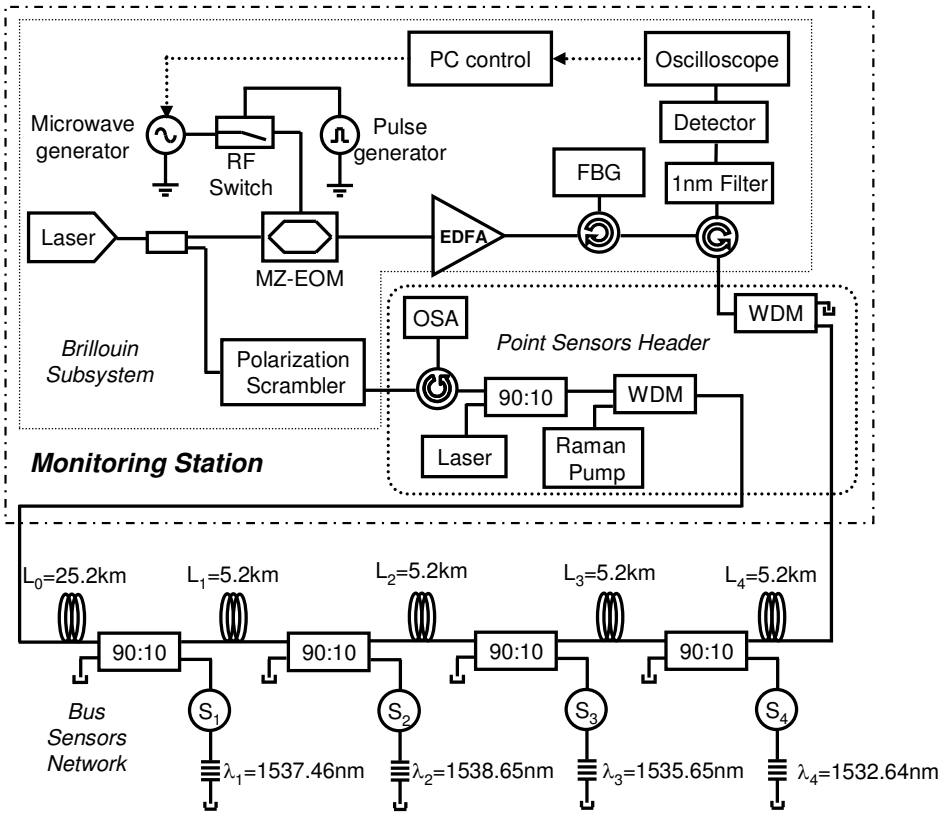

Fig. 1. Hybrid sensor network with point and distributed optical sensors. The monitoring station includes the Brillouin subsystem and the point sensors header.

The sensor network has a bus topology with a total length of 46 km of standard single mode fiber (SSMF). Individual point sensors are introduced in the network by the use of fiber couplers. A dual-ended approach is implemented because of the Brillouin distributed sensing scheme deployed in the network. However, the network could be transformed to single-ended measurements by deploying well-known techniques [14]

The monitoring station is where the signals needed for interrogation of the point sensors and for the Brillouin distributed measurements are generated. The Brillouin measurement system is based on the Brillouin optical time-domain analysis (BOTDA) principle in which a pulsed pump and a continuous (CW) Stokes waves counterpropagate in the fiber under test. This kind of Brillouin distributed sensors offer the best dynamic ranges for long-length measurements and it can provide strain as well as temperature measurements. The details of the optimized implementation that we deploy are given in section 2.1

The bus topology was used for wavelength-division multiplexing (WDM) the point sensors. We demonstrated the use of four sensors. Each one incorporates a narrow-bandwidth FBG at a unique wavelength. The launched signals are ultimately incident on all of the sensors but the gratings ensure that each sensor returns only its characteristic channel towards the launching point (the head end) after passing through the sensor a second time. The specific sensors used, S_1, S_2, S_3 and S_4 in Fig. 1, were vibration sensors based on fiber optic taper sensors as explained in section 2.2.

A Raman pump laser is also deployed at one of the fiber outputs of the monitoring station in order to generate distributed amplification in the sensor bus extending the fiber sensor network range. This pump laser is injected into the fiber bus by using a fiber wavelength

#123929 - $15.00 USD Received 8 Feb 2010; revised 6 Apr 2010; accepted 6 Apr 2010; published 22 Apr 2010

division multiplexer. Another wavelength division multiplexer is used at the other end of the bus to prevent the residual Raman pump from re-entering the monitoring station.

2.1 Brillouin distributed sensing subsystem

In this network we deploy a novel setup for BOTDA which is optimized for long-range measurements [15]. The needs of long-range BOTDA systems differ significantly from those focused on short-distance high-resolution measurements. Their main limitations come from the so-called non-local effects. These are caused by depletion of the pump pulse as it amplifies the CW probe signal along the fiber [16]. This depletion makes the Brillouin spectra measured in a particular position of the fiber dependent on the Brillouin interaction in all preceding locations, thus introducing systematic errors in measurements. The errors increase with fiber length and also pump power.

Furthermore, in long-range BOTDA sensors the problem of non-local effects is greatly enhanced by the use of pump pulses with insufficient extinction ratio (ER). The DC baseline of the pulse also interacts with the CW probe signal amplifying this signal through Brillouin interaction and severely distorting the measured spectra. Moreover, amplification of the CW leads to increased depletion of the pump and the worsening of measurement errors. Therefore, generating pump pulses with very high extinction ratio is of the essence. In most BOTDA setups pump pulses are shaped by using electro-optic modulators (EOM) [17]. However, standard EOMs typically have ER in the 20 dB to 30 dB range, which is insufficient to avoid non-local effects and distortion of the measured spectra. An alternative is to use specialty EOMs specially design for enhanced ER. However, these are costly devices. Ideally, standard EOMs with the economies of scale associated to telecom-grade devices should be usable.

In this network we deploy a novel method to generate pump pulses with ultra-high ER using standard low-ER EOM [15]. It is based on shaping the pulses in the electrical instead of the optical domain. As it is shown in Fig. 1, the signals for Brillouin distributed sensing are obtained from a common laser. The output of this laser is divided in two branches: upper branch, where the pump pulses are generated and lower branch, where the probe signal is obtained.

The pump pulses are first generated in the RF domain. The output of a microwave generator with output frequencies close to the Brillouin frequency shift is applied to the input of an RF switch, which is driven by a pulse generator. Commercial RF switches are available that have extremely high isolation, typically between 60dB and 80dB. Therefore, at the output of the RF switch we get short pulses of RF energy with equivalently high extinction ratio. Next step is translating these pulses to the optical domain. This is performed by using optical single-sideband (OSSB) modulation. A Mach-Zehnder electro-optic modulator (MZ-EOM) is driven by the RF pulses and biased at minimum transmission in order to generate optical double-sideband suppressed-carrier (ODSB-SC) modulation. Then, a fiber Bragg grating filter is used to remove one of the sidebands; hence, we end up having a pulsed optical single-sideband suppressed-carrier modulation. The characteristics of the RF pulse are directly translated to the optical domain by this modulation format and consequently optical pump pulses with 60-dB to 80-dB extinction ratio and tunable wavelength are obtained. The Brillouin spectra along the fiber are scanned by tuning microwave generator frequency. Finally the pump signal is injected in the sensor bus.

In the lower branch of the setup the probe signal is simply polarization scrambled so as to avoid Brillouin polarization dependencies and then it is also injected in the sensor network. The probe signal counter-propagates with the pump pulses in the network and finally arrives back to the detection system, where it is captured using a photoreceiver and digital high-speed scope. The photoreceiver is preceded by a 1-nm wide optical filter tuned to the wavelength of the Brillouin signals that is inserted to avoid any crosstalk from the point sensors interrogation system. The operation of the microwave and pulse generators is controlled by a computer that is also used to acquire and process the measured signals.

#123929 - $15.00 USD Received 8 Feb 2010; revised 6 Apr 2010; accepted 6 Apr 2010; published 22 Apr 2010

One way to enhance the measurement range in BOTDA sensors is by increasing the pulse pump power so as to increase the CW probe signal gain. However, this is limited by the onset of the modulation instability (MI) effect [18], which limits the maximum usable power. Recently the use of optical pulse coding has been proposed to increase the measurement dynamic range; thus avoiding the need for high pump powers [19,20]. Another method to enhance the length of Brillouin distributed sensors is by using Raman amplification. This has the main advantage that the gain is distributed along the fiber so that the pump pulse does not reach at any position the high power that causes the MI effect.

The use of Raman amplification has been demonstrated for the Brillouin Optical Time-domain Reflectometer type sensor [6]. However, to our knowledge it has never been experimentally demonstrated in BOTDA sensors although its use has been proposed [21]. In our system, we deploy Raman distributed amplification for backward pumping of the pump pulses and forward pumping of the probe.

2.2 Point sensors network subsystem

In this work, it is also demonstrated a WDM network for point sensors multiplexing over the same 46 km of the single mode fiber used for distributed sensing. The network has a distributed fiber Raman amplified bus topology which includes four directional couplers along the 46 km of the sensing fiber in order to multiplex four vibration sensors. The sensors are WDM addressed by four Fiber Bragg gratings (FBGs) and it is possible to measure their intensity variations by use of a Raman pump laser to obtain enough amplification.

The original setup was the bus topology shown in [13] for a shorter length (35 km), with an active bus built on SSMF (ITU-G.652 compliant). Although it has a relatively low Raman efficiency (due to its large effective area), it is widely used in telecommunications networks, where the influence of impairments such as nonlinear cross-talk and Rayleigh back-scatter is low, as well as its cost.

The Raman pump, signal(s) and receiver are co-located in one head end. This strategy would remove the logistical inconvenience of electrical power feeds to remote locations. The Raman pump propagated co-directionally with the launched signal but counter-directionally with the returned signals from the gratings. Pumping from the opposite end of the bus (or even bi-directional pumping) is also possible.

Directional couplers (90:10 ± 0.3% ratios) at the pump and all signal wavelengths are shown in Fig. 1 to perform power distribution among the sensors. Their insertion losses vary from 10.4 dB to 10.8 dB in the 10% branch for the pump and the signal wavelengths and from 0.5 dB to 0.7 dB in the 90% branch for the pump and the signal wavelengths. 5.2-km fiber spans are placed between the couplers. However, there is no strict constraint on the lengths. (Indeed, greater spans would enable improved pumping efficiency).

All of the free terminations on the bus are refractive-index-matched to frustrate unwanted reflections. This is of particular importance to minimize multi-path interference [22]. The signal source used to interrogate the point sensors is a tunable laser (1460 - 1580 nm) with a spectral linewidth of 5 MHz. The Raman amplification is provided by a pump laser that it is able to couple up to 3.2 W into the single-mode fiber at 1445 nm.

The peak wavelengths of the gratings are marked on Fig. 1. The grating wavelengths corresponded to frequency shifts from the pump ranging between 11.7 and 12.8 THz. These values are selected so as to be on the short wavelength side of the peak of the Raman gain profile (which is ~13.2 THz from the pump in the germano-silicate glass of standard single mode fiber). By making such a choice, the Raman gain profile increases with frequency shift. This property is used to obtain a degree of power equalization of the returned signals from the sensors.

From [23], it is known that Raman amplification is oriented to long-range bus networks. Therefore, the first span of 25.2 km of standard single mode fiber acts as an amplification

#123929 - $15.00 USD Received 8 Feb 2010; revised 6 Apr 2010; accepted 6 Apr 2010; published 22 Apr 2010

span to maximize the Raman gain in the bus. However, it is also possible to locate sensors closer to the header if necessary [12].

In the sensor network used within this work the pump power to obtain equalization of the four sensors using Raman amplification is 1 W, which is also a good compromise for the amplification of the Brillouin signals as described below. The four output reflected signals from the FBGs are equalized at −23 dBm, and the maximum peak difference between the four channels is approximately 0.29 dB. Figure 2 displays the complete measured spectrum for the four sensors using Raman amplification. It is also represented the peak power of the optical output signal, at the Brillouin amplified wavelength.

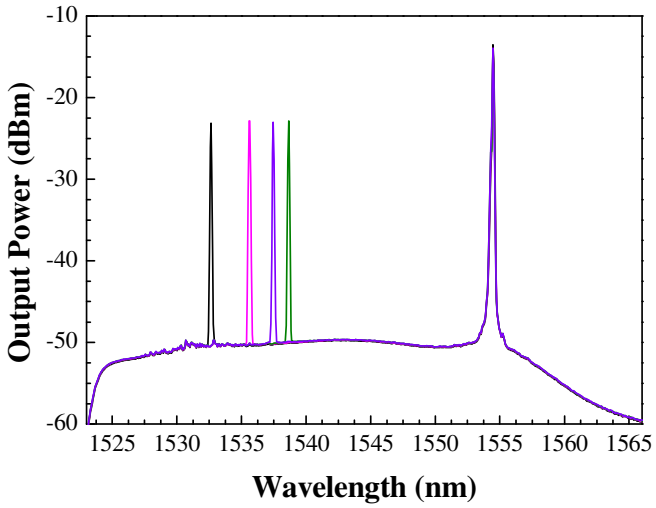

Fig. 2. Measured optical spectrum for the four point sensors and the Brillouin + Raman amplified transmitted signal.

As it was mentioned before, four point vibration sensors are multiplexed along the network. They are based on fiber-optic taper sensors employed as transducers to measure mechanical vibrations. They show some advantages, as their simple fabrication process, low-cost and versatility in the number of measurable parameters [24]. The tapers were implemented by elongating the fiber during a fusion process, inducing insertion losses (more details can be found in [8], [10] and [25]). The transmitted optical power of the taper depends on its bending radius: as it decreases, the transmitted power decreases as well [8], so it can be used to detect vibrations just by monitoring the power variations [24]. In this case, the optical signal crosses the taper back and forth, because the sensors are used in reflective configurations. Thus, they have double sensitivity, although the losses are also doubled. So, there must be a compromise between the sensors' sensitivity, the induced losses and the maximum measuring length.

3. Experimental results and discussion

We assemble a proof-of-concept experiment in order to demonstrate the hybrid network concept following the design explained in previous section. The 46-km bus length was implemented in the experiments using SSMF: one 25.2-km reel plus four 5.2-km reels. Four point sensors were located at 5.2-km intervals at the end (from the point of view of the interrogation system) of the fiber bus in order to simulate a worst-case scenario. A length of 200 m of fiber round the middle of the fiber bus (at 25.2-km distance from the Brillouin pump input) is inserted in a temperature-controlled climatic chamber at 60°C.

#123929 - $15.00 USD Received 8 Feb 2010; revised 6 Apr 2010; accepted 6 Apr 2010; published 22 Apr 2010

3.1 Brillouin distributed temperature measurements

In the Brillouin distributed system we deployed a 1550-nm laser with an 100-KHz line-width and 0.5-pm stability. The pump power before Raman amplification was 18 dBm and the CW probe was −20 dBm. 130-ns pump pulses were used; hence the spatial resolution of the measurements was 13m. This was only limited by the speed of the RF switch that we had available. The use of faster devices that are commercially available would provide higher resolutions.

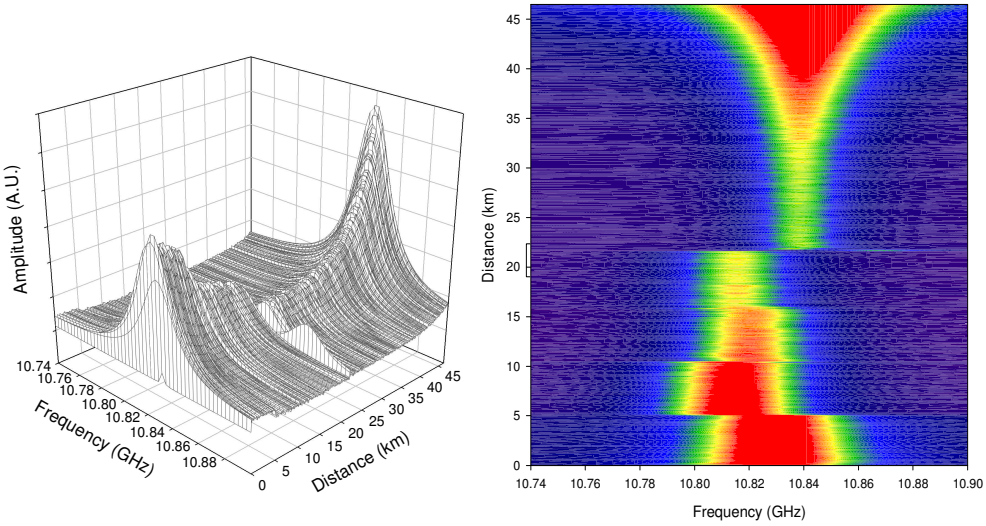

a) b)

Fig. 3. Measurement of Brillouin gain spectra along the fiber network. a) 3D representation. b) intensity plot representation.

Figure 3 displays the complete characterization of the Brillouin spectra along the fiber. Figure 3(b) depicts an intensity plot in which higher amplitude of the spectra is depicted as brighter colors. It can be appreciated that the five fiber reels that make the bus have slightly different intrinsic Brillouin frequency shift. This is attributed to different compositions (as they come from 2 different vendors) and winding tensions. The heated fiber in the middle of the bus is also distinguished. Figure 1(a) depicts a 3D view of the Brillouin spectra that highlights their amplitude evolution along the fiber, which is directly linked to the pump pulse amplitude that the probe wave finds at each location. The amplitude of the pulses start to decay due to fiber attenuation as they start to travel through the fiber, but round the middle of the bus the trend is inverted and the amplitude progressively increases until the fiber bus end. This behavior is due to Raman pump. We analyzed various pumping configurations to find that backward Raman pumping of the pump pulses was optimal. The reason is that in this way the pump pulses get maximum amplification when it is most needed, i.e., at the end of their journey through the fiber. This explains the observed trend-change at the middle of the fiber bus. With this configuration the worst case location for Brillouin measurements is the middle of the fiber sensor bus. Therefore, as it is shown below, we referred our measurement resolution results to that location. The optimum Raman pump was found to be 1 W. The use of higher pumps increased the probe wave amplitude too much leading to significant saturation of Brillouin gain and depletion of the pump, which introduced systematic measurement errors. In a network with more point sensors the Raman pump would be increased accordingly to compensate the additional coupler losses.

Figure 4 depicts the measurements of Brillouin frequency shift along the fiber that was obtained by post-processing the data in Fig. 3. Figure 4(a) highlights the four initial 5.2-km

#123929 - $15.00 USD Received 8 Feb 2010; revised 6 Apr 2010; accepted 6 Apr 2010; published 22 Apr 2010

reels with slightly different Brillouin frequency shift, then the temperature-controlled 200-m length and finally the rest of the 25.2-km reel. Figure 4(b) zooms on the temperature controlled area. The Brillouin frequency shift in this area was measured to be 10.868 GHz which agreed with a previous calibration of the fiber that had given a temperature coefficient of 0.9 MHz/°C. The standard deviation of the measurement in the 200-m heated fiber was of 0.6 MHz. Hence the temperature resolution of the measurements was estimated to be 0.7°C.

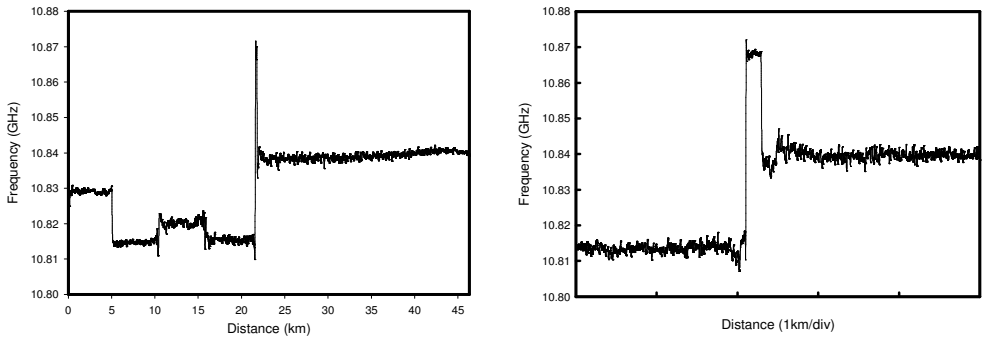

a) b)

Fig. 4. Brillouin frequency shift distribution along the fiber.

3.2 Point sensors measurements

In this section, we describe the sensors configuration and the measurements obtained utilizing them inside the multiplexing network. The fiber-optic sensors were fabricated using a splicing machine with a modified program to move one of the arms trapping the fiber while the fusion happens. The arc fusion power and the splicing time were fixed to have tapers with different elongations, depending on the moveable arm length. Obviously, as the length increased, the sensor would have higher loss and sensitivity, and consequently, it would be more fragile.

When vibration is applied to these taper sensors, the fiber is bent in the stretched area, giving a curvature's change, and then, a variation in the transmitted power. To characterize the sensors' response, we applied vibrations of different frequency, amplitude and waveform. The applied frequencies ranged from 0.1 Hz to 100 Hz and the amplitudes varied from 0.5 mm to 3.25 mm (limited by the variable frequency mechanical wave driver from Pasko, mod. SF-9324 utilized in our experiments).

The main design parameter of the point sensors was the loss induced by the taper, which determined the sensitivity and the dynamic range. It was optimized so that the maximum losses induced by the sensors were 1.75dB, which were doubled in the experimental set up because the signal passes through each sensor twice.

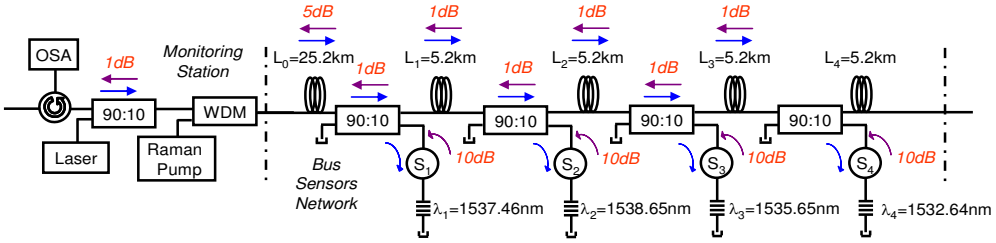

Fig. 5. Insertion losses present in sensors network.

Figure 5 shows the losses present in the remote sensing network. By using Raman amplification, the limitation in the maximum sensing length is not due to signal attenuation,

#123929 - $15.00 USD Received 8 Feb 2010; revised 6 Apr 2010; accepted 6 Apr 2010; published 22 Apr 2010

but because of Rayleigh backscattering. When a sensor is located further from the head of the network, the noise level increases, and the signal coming from the sensor is attenuated by the length travelled, the taper's loss, the 90:10 coupling ratios and the grating's reflectivity. The most critical measurement corresponds to the sensor located in the further position, because of both the attenuation suffered and the Rayleigh backscattering. The dynamic range (the measurable optical power variations) was improved using Raman amplification (with 1W pump power), giving a value of 3 dB in the worst case. For the nearest sensor, the dynamic range was higher than 10 dB.

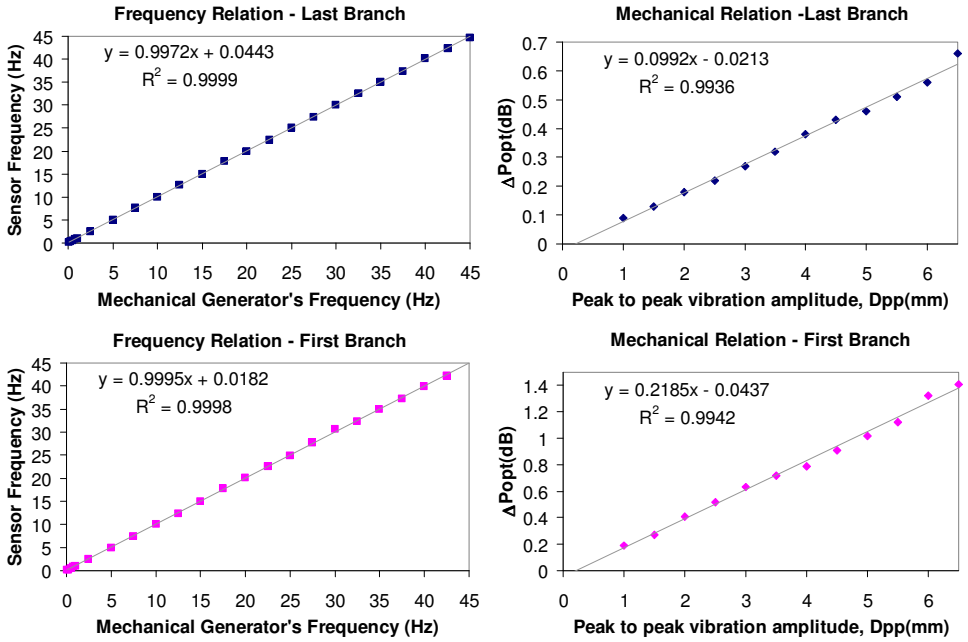

Fig. 6. Sensor's frequency and amplitude responses (first and second column respectively) for the first and last vibration sensors.

The sensor characterization was performed regarding two main parameters: frequency and amplitude response. To measure the frequency response, a sinusoidal wave with 6.5 mm peak-to-peak variation at different frequencies was applied, aiming to check if the returned signal from the sensor had the same shape and frequency than the excitation signal. Figure 6 displays the results obtained. In both cases, the sensor's frequency equals the mechanical generator's frequency. To analyze the amplitude response, a 45 Hz vibration frequency was used and the amplitude was varied from 6.5 mm peak-to-peak to 1 mm peak-to-peak. As before, there was a lineal relation between the vibration amplitude applied and the returned sensor's optical power amplitude (Fig. 6). The vertical axis of the right column charts are not the same. The difference between these ranges is due to the effect of Rayleigh back scattering: as the distance increases, it does so, overlapping the dynamic range of the sensor. This lowers the final sensibility of the last sensor, but anyway, the system is able to measure the same amplitude range as the sensor placed in the first branch.

Nowadays, the commercial equipment used to measure vibrations works with specific units that combine the spectral response and the amplitude variation, *mm/s RMS*, measuring the vibration's velocity. The measurable range with the obtained parameters for frequency vibrations between 0.1 Hz and 100 Hz was:

#123929 - $15.00 USD Received 8 Feb 2010; revised 6 Apr 2010; accepted 6 Apr 2010; published 22 Apr 2010

$$V_{RMS-Min} = 0.22\ mm/s\ RMS$$
$$V_{RMS-Max} = 650\ mm/s\ RMS \quad (1)$$

4. Conclusions

This work contributes to the development of the large scalable networks of sensors that are required to monitor extended infrastructures in many practical applications. A 46-km hybrid network that demonstrates a novel cost-effective architecture that integrates point and distributed Brillouin sensors and uses Raman amplification has been implemented for the first time to our knowledge. The use of Raman amplification in BOTDA distributed sensors, which is also demonstrated for the first time, serves to compensate branching and fiber losses in the network and provides a good temperature resolution of 0.7°C and a spatial resolution of 13 m. This performance can be improved by fine tuning of the system; particularly the substitution of the RF switch with a faster device would provide meter or even sub-meter resolution. Furthermore, the simultaneous Raman amplification of the signals from the low-frequency (from 0,1 to 50 Hz) vibration point sensors allows theme to be placed as far away as the end of the fiber bus, 46 km away from the interrogation equipment overcoming low power levels or backscattering noise problems.

Acknowledgements

The authors would like to acknowledge the financial support from the Spanish Ministerio de Educación y Ciencia through project TEC2007-67987-C02-02.

#123929 - $15.00 USD Received 8 Feb 2010; revised 6 Apr 2010; accepted 6 Apr 2010; published 22 Apr 2010